Available online at www.sciencedirect.com
SCIENCE DIRECT
Earth and Planetary Science Letters 248 (2006) 286–300
EPSL
www.elsevier.com/locate/epsl

Subduction-related origin of the 750 Ma Xuelongbao adakitic complex (Sichuan Province, China): Implications for the tectonic setting of the giant Neoproterozoic magmatic event in South China

Mei-Fu Zhou [a,*], Dan-Ping Yan [b], Chang-Liang Wang [b], Liang Qi [a], Allen Kennedy [c]

[a] *Department of Earth Sciences, University of Hong Kong, Hong Kong, China*
[b] *State Key Laboratory of Geological Processes and Mineral Resources, China University of Geosciences, Beijing 100083, China*
[c] *SHRIMP II Laboratory, Curtin University of Technology, Perth, Australia*

Received 30 November 2005; received in revised form 28 April 2006; accepted 26 May 2006
Available online 3 July 2006
Editor: V. Courtillot

Abstract

The Xuelongbao plutonic complex in the eastern margin of the Tibetan Plateau is dated at 748±7 Ma using the SHRIMP zircon U–Pb method and represents part of the Neoproterozoic igneous assemblage of South China. Rocks in the complex include tonalite and granodiorite and have SiO_2 ranging from 62.0 to 74.8 wt.% and Al_2O_3 from 14.3 to 20.9 wt.%. Their Na_2O contents range from 4.2 to 6.7 wt.% and K_2O from 0.47 to 1.96 wt.%, indicating that they belong to the Na-series. These rocks show chondrite-normalized REE patterns depleted in HREE and variably enriched in LREE. They have positive Sr and negative Nb and Ti anomalies in the primitive mantle-normalized trace elemental spider diagram. Their Sr contents range from 320 to 780 ppm and Y contents are lower than 10 ppm, resulting in high Sr/Y ratios (52–320), characteristic of typical adakites. Their εNd (*t*) and initial Sr isotopic compositions range from +0.36 to +2.88 and from 0.7033 to 0.7054, respectively. The geochemical features of the Xuelongbao plutonic complex are consistent with an origin from adakitic magmas that were likely derived from partial melting of a subducted oceanic slab. Together with arc signatures of other granites and mafic intrusions in the region, the 750 Ma Xuelongbao adakitic complex provides evidence for a major, subduction-related Neoproterozoic magmatic event of South China.

Keywords: Neoproterozoic; dating; subduction; adakitic magma; granitoid; South China

1. Introduction

The extensive Neoproterozoic magmatism in South China, known as the Jinningian magmatism [1], resulted in the formation of voluminous igneous rocks around the Yangtze Block. These igneous rocks have been interpreted by some as the result of a mantle plume associated with the break-up of Rodinia [2,3]. Others suggested that they formed in two major arcs around the Yangtze Block: the Jiangnan arc to the east [4,5] and the Hannan-Panxi arc to the west [6–8]. Although the rocks have clear arc geochemical signatures, these signatures could also reflect inherited features of crustal rocks or subduction-modified mantle sources. Therefore, the origin of the giant Jinningian magmatism in South China is still enigmatic, despite its extreme importance in understanding the tectonic evolution of South China.

* Corresponding author. Tel.: +852 2857 8251; fax: +852 2517 6912.
E-mail address: mfzhou@hkucc.hku.hk (M.-F. Zhou).

0012-821X/$ - see front matter © 2006 Elsevier B.V. All rights reserved.
doi:10.1016/j.epsl.2006.05.032

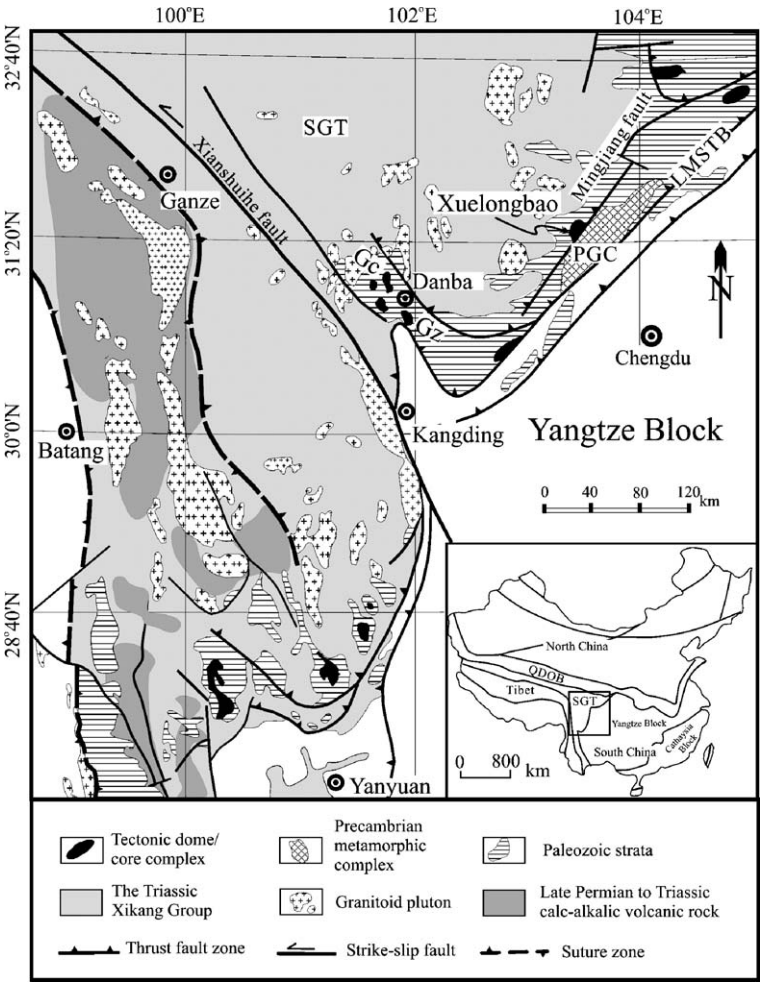

Fig. 1. Regional geological map showing the location of the Xuelongbao dome in the eastern margin of the Tibetan Plateau [modified from [6,26]]. SGT = Songpan-Ganze terrane; QDOB = Qilin–Dabie orogenic belt; LMSTB = Longmenshan Thrust Belt; Gc =Gongcai complex; Gz = Gezhong complex; PGC = Pengguan complex.

Adakite is an intermediate to acidic volcanic rock with relatively low K and high Al and Na contents. It may have moderate or high Sr and is depleted in Y and HREE [9,10]. Such rocks form in arc settings related to subduction of an oceanic slab [11–13] or in the lower part of a thickened crust [14–17]. Plutonic grantoids derived from adakitic magmas have also been reported in several localities [18–25]. Here, we report adakitic affinities in plutonic rocks of the Xuelongbao tectonic dome, one of the domes emplaced along the eastern margin of the Tibetan Plateau. These domes represent the Neoproterozoic igneous assemblage of the Yangtze Block. The plutonic complex is composed of tonalite and granodiorite, and has a SHRIMP zircon U–Pb age of 748±7 Ma, making it contemporaneous with the Jinningian magmatism of South China. This paper describes the Xuelongbao complex and presents new geochemical data that support its adakitic affinity. Based on whole-rock major and trace elemental data and Sr–Nd isotopic analyses, we propose that the plutonic rocks in Xuelongbao were derived from adakite-like magmas formed by partial melting of an oceanic slab (slab melting). The identification of Neoproterozoic adakitic rocks provides for the first time convincing evidence that the giant Jinningian magmatism in South China was formed in a subduction-related environment.

2. Geological background

South China comprises the Cathysian Block to the southeast and the Yangtze Block to the northwest (Fig. 1). The Yangtze Block consists of Precambrian metamorphic complexes overlain by a thick (>10 km) sequence of late Neoproterozoic (Sinian) to Cenozoic cover rocks. The crystalline rocks include paragneiss, mica schist, graphite-

bearing sillimanite–garnet gneiss (khondalite), amphibolite, marble, and quartzite. The cover sequence is composed of clastic, carbonate, and metavolcanic rocks [27].

The easternmost part of the Tibetan Plateau is marked by the Longmenshan Thrust Belt that separates the Yangtze Block to the east and the Songpan-Ganze Terrane to the west (Fig. 1). The Songpan-Ganze Terrane is characterized by a thick sequence of Triassic strata (ca. 7 km) of deep marine deposits, known as the Xikang Group [27–29]. Internally, the Xikang Group was intensely deformed by folding and thrusting during the Late Triassic and Early Jurassic in the Longmenshan Thrust Belt [28]. This deformational event was possibly contemporaneous with collision and subsequent continuing convergence between North and South China [28]. Clockwise rotation of the eastern part of the Songpan-Ganze Terrane was associated with movement along the Xianshuihe fault during the India–Eurasia collision, causing the Cenozoic Longmenshan Belt to be thrust onto the Sichuan basin (see reviews in [29]). In the eastern part of the Songpan-Ganze Terrane, the Xikang Group is conformably underlain by Palaeozoic shallow marine sequences of South China [28].

The Palaeozoic strata and Triassic sequence are intruded by abundant Mesozoic granitic plutons (Fig. 1).

Crystalline basement rocks of the Yangtze Block are exposed as tectonic domes surrounded by Sinian through Permian units. Around these domes, stratigraphic sequences were removed or significantly thinned [26,27]. Thus, the domes are extensional features formed by SSE extension probably at around 170 Ma [6,26]. The Xuelongbao dome in the Longmenshan Thrust Belt is one of these tectonic domes emplaced along the eastern margin of the Tibetan Plateau (Figs. 1 and 2).

3. Geology of the Xuelongbao dome

The Xuelongbao dome is similar to the Gezong plutonic dome in the Danba area, southwest of Longmenshan [6] and is composed of a plutonic complex as the inner core, surrounded partly by a schist complex known as the

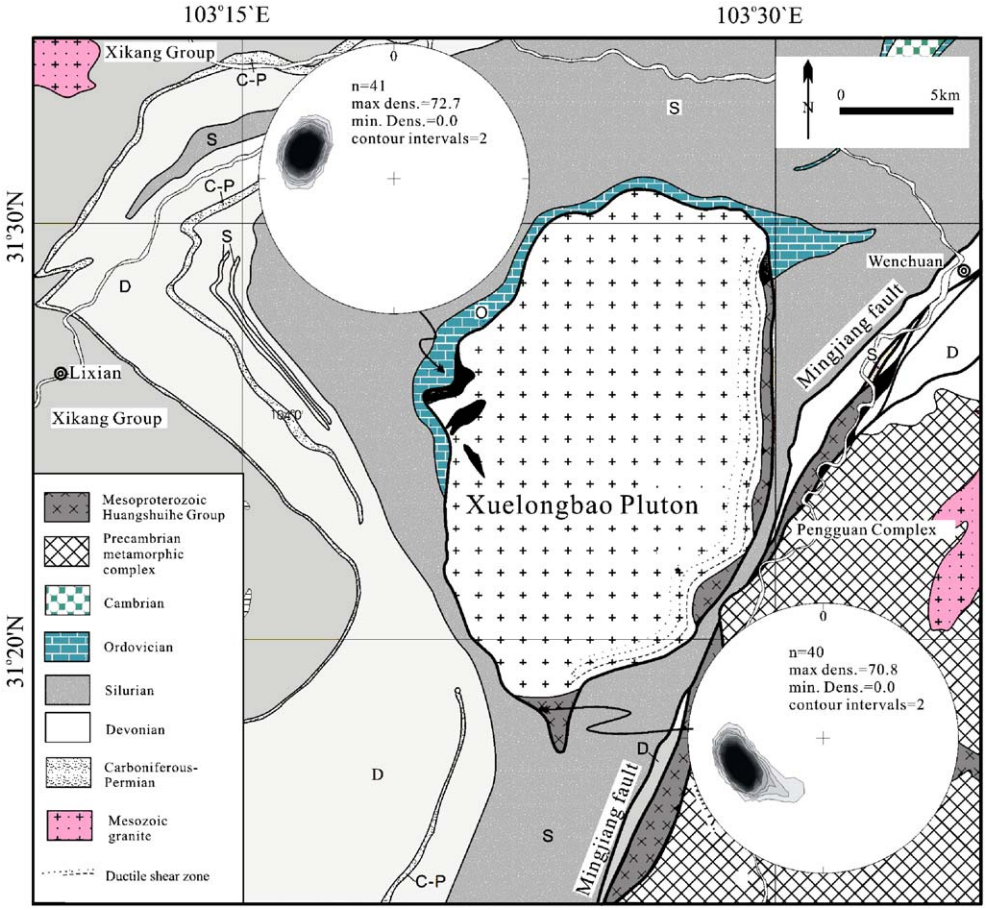

Fig. 2. Geological map of the Xuelongbao dome, Sichuan Province, SW China [modified from [27]]. Inset maps show the projection of lineations along the basement detachment fault and hanging wall of ductilely deformed rocks (equal area projection, lower hemisphere).

Huangshuihe Group and locally by Palaeozoic strata (Fig. 2). The Xuelongbao complex crops out over an area of 236 km^2 and forms a crude NNE-striking ellipse. Both the granitic complex and Huangshuihe Group form the core complex which is separated from the Paleozoic strata by a ductile, basement detachment fault. Within this detachment fault, there is a well-developed S-C fabric and mineral lineation, orientated roughly east–west (insets in Fig. 2).

The plutonic rocks show intrusive contact with the Huangshuihe Group. The Huangshuihe Group consists of quartz–mica schist and amphibolite with a Mesoproterozoic protolith age [27]. The Paleozoic sedimentary sequence includes Ordovician, Silurian, Devonian, Carboniferous and locally Permian strata and is identical to that of the Yangtze Block. To the west the Mesozoic strata belong to the Triassic Xikang Group. These sequences were intruded by Mesozoic granites (Figs. 1 and 2).

The Xuelongbao dome is separated from the adjacent Pengguan complex by a NE-striking Mingjiang fault, a part of the Longmenshan Thrust Belt (Figs. 1 and 2). Both the Xuelongbao and Pengguan complexes were involved in the southeastward-directed Longmenshan overthrust.

The Xuelongbao plutonic complex is composed of coarse-grained biotite tonalite in the centre, mantled by finer-grained biotite granodiorite, and then two-mica granodiorite. In the marginal zone, xenoliths of diorite and metamorphic rocks of the Huangshuihe Group have been aligned by a magmatic flow. Major minerals of the plutonic rocks include plagioclase (50–70%), K-feldspar (<10%), quartz (20–30%) and biotite (5–10%).

4. Analytical methods

U–Pb isotopic ratios of zircon separates were measured using the sensitive high-resolution ion microprobe (SHRIMP II) at Curtin University of Technology in Perth, Western Australia. The measured isotopic ratios were reduced off-line using standard techniques. The U–Pb ages were normalized to a value of 564 Ma determined by conventional U–Pb analysis of zircon standard CZ3. Common Pb was corrected using the method of Compston et al. [30]. The $^{206}Pb/^{238}U$ and $^{207}Pb/^{235}U$ data were corrected for uncertainties associated with the measurements of the CZ3 standard and the $^{206}Pb/^{238}U$ and $^{207}Pb/^{235}U$ ages were normalized to the results of the standard analyses. The $^{207}Pb/^{206}Pb$ ages given in Table 1 are independent of the standard analyses.

Major oxides were determined by wavelength-dispersive X-ray fluorescence spectrometry (WD-XRFS) of fused glass beads using a Philips PW2400 spectrometer at the University of Hong Kong. Trace elements were determined by inductively-coupled plasma mass spectrometry (ICP-MS) of nebulized solutions using a VG Plasma-Quad Excell ICP-MS also at the University of Hong Kong after a 2-day closed beaker digestion using a mixture of HF and HNO_3 acids in high-pressure bombs [31]. Pure elemental standard solutions were used for external calibration and BHVO-1 (basalt) and SY-4 (syenite) were used as reference materials. The accuracies of the XRF analyses are estimated to be ±2% (relative) for major oxides present in concentrations greater than 0.5 wt.%. The accuracies of the ICP-MS analyses are estimated to be better than ±5% (relative) for most elements [31].

Rb–Sr and Sm–Nd isotopic analyses were performed on a VG-354 thermal ionization magnetic sector mass spectrometer at the Institute of Geology and Geophysics, Chinese Academy of Sciences, Beijing. Mass fractionation corrections for Sr and Nd isotopic ratios were based on values of $^{86}Sr/^{88}Sr=0.1194$ and $^{146}Nd/^{144}Nd=0.7219$. Uncertainties in Rb/Sr and Sm/Nd ratios are less than ±2% and ±0.5% (relative), respectively [32].

Table 1
SHRIMP zircon U–Pb analytical results for a tonalite from the Xuelongbao dome, Sichuan, SW China

Spot	Concentration (ppm)				$^{232}Th/^{238}U$	Age (Ma)						
	Common ^{206}Pb	U	Th	Radiogenic ^{206}Pb		$^{206}Pb/^{238}U$	1δ	$^{207}Pb/^{206}Pb$	1δ	$^{208}Pb/^{232}Th$	1δ	% Discordant
XL-20-1	0.06	322	443	33.7	1.42	740.9	9.2	773	14	727	13	4
XL-20-2	0.15	150	164	14.9	1.13	704.4	9.2	741	35	722	12	5
XL-20-3	0.9	57	40	6.7	0.72	820.7	15.1	646	62	762	27	−21
XL-20-4	0.02	447	112	48	0.26	759.7	9.3	783	12	749	13	3
XL-20-5	0.26	60	30	6.2	0.52	723.9	12.5	796	70	704	29	10
XL-20-6	−0.22	78	49	8.2	0.65	743.8	12.9	847	34	773	23	14
XL-20-7	0.03	359	259	38	0.75	750.3	9.3	821	15	744	11	9
XL-20-8	0.13	96	44	10.1	0.47	738.7	10.2	707	43	731	23	−4
XL-20-9	0.28	138	89	14.6	0.67	748.1	9.7	665	30	730	13	−11
XL-20-10	0.27	46	4	4.8	0.1	744.5	11.4	736	84	630	155	−1
XL-20-11	−0.04	109	31	11.7	0.3	758.4	10.1	781	25	780	18	3
XL-20-12	0.17	66	33	7	0.52	751.2	11	741	48	741	24	−1

5. Analytical results

5.1. Crystallization age of the Xuelongbao plutonic complex

Numerous zircon grains were separated from a tonalite (sample XL-20) of the Xuelongbao dome, composed of plagioclase, quartz, K-feldspar and biotite. Zircons from this sample exhibit a wide spectrum of crystal morphologies including sector zoned, subequant zircons and oscillatory zoned zircons. Some zircons may have inner cores (Fig. 3), suggesting an igneous origin with some inherited cores.

One analysis of a core in a sector zoned zircon grain yielded a slightly older $^{206}Pb/^{238}U$ age of 821±15 Ma (analysis 3) (Table 1), interpreted to be xenolithic in origin. An overgrowth on a zircon grain (Fig. 3) has a younger $^{206}Pb/^{238}U$ age of 704±9 Ma (analysis 2) (Table 1). These two analyses are rejected in the final calculation. The other 10 analyses of zircons with a variety of morphologies gave concordant ages that yield an average $^{206}Pb/^{238}U$ age of 748±7 Ma (Fig. 4). The chi-squared values for this single cluster of analyses is 1.2, indicating that this group is a single population. There is no apparent relationship between age and U content. The data for this sample are consistent with the zircons being from a magmatic source.

5.2. Whole rock major element oxides

Rocks from the Xuelongbao complex show large variations in whole-rock chemical compositions. Their SiO_2 contents vary from 62 to 74.8 wt.%, Al_2O_3 from 14.3 to 20.9 wt.%, and MgO from 0.21 to 2.4 wt.% (see Table 2).

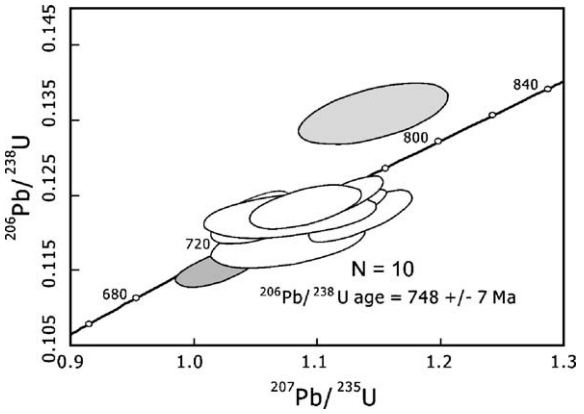

Fig. 4. SHRIMP zircon U–Pb concordia plot for the tonalite sample (XL21) from the Xuelongbao dome, SW China. Shaded blocks are analyses that are not included in the age calculation.

Based on their CIPW normative minerals, they fall in the field of granodiorite, tonalite and diorite on an alkali feldspar–quartz–plagioclase diagram (Fig. 5a) or trondhjemite and tonalite on an Ab–An–Or diagram (Fig. 5b), similar to Archaean tonalite–trondhjemite–granodiorite (TTG) suites and adakite [9]. They have total alkalis (Na_2O+K_2O) ranging from 6 to 10 wt.%, but have much lower K_2O contents (0.47 to 1.96 wt.%) than Na_2O contents (4.2 to 6.7 wt.%) and small K_2O/Na_2O ratios (<0.34, mostly <0.25), indicating that they belong to the Na-series (Fig. 6a). In the plots of SiO_2 vs. MgO (Fig. 6b), Xuelongbao samples are similar to the high-Si adakites and completely different from the low-Si adakites as defined by Martin et al. [9]. They also have relatively high Mg#s (0.34 to 0.50) (Table 2).

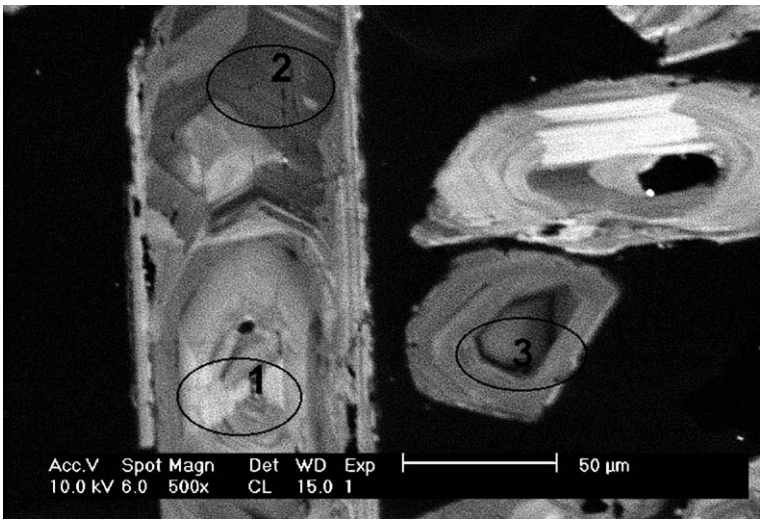

Fig. 3. Catholuminusence photo of zircon grains in the tonalite sample, XL21, from the Xuelongbao complex, SW China, showing igneous zoning. Circles are the spots of the SHRIMP analyses.

Table 2
Major oxides and CIPW norms of the plutonic rocks from the Xuelongbao dome, SW China

	XL-4	XL-6	XL-7	XL-19	XL-20	XL-21	XL-25	XL-26	XL-28	XL-29	XL-34	XL-35	XL-36	XL-38	XL-67	XG-1	XG-2	XG-3	XG5-1	XG5-2	XG5-3	XG-6	XG-7
Major oxides (wt.%)																							
SiO_2	66.8	67.0	68.2	66.8	71.0	62.0	70.1	72.0	67.5	71.1	65.3	66.5	65.6	65.7	68.0	64.5	67.5	65.2	64.8	74.8	65.1	65.7	65.9
TiO_2	0.36	0.31	0.30	0.28	0.15	0.49	0.22	0.12	0.34	0.11	0.26	0.26	0.36	0.35	0.32	0.39	0.31	0.39	0.47	0.08	0.44	0.37	0.42
Al_2O_3	17.76	17.20	16.83	17.66	16.88	17.07	15.60	16.35	16.39	16.10	17.75	17.41	17.46	17.31	16.61	17.32	16.56	16.99	16.05	14.33	16.42	17.04	16.61
Fe_2O_3	3.35	2.89	2.62	3.07	1.81	5.09	2.12	1.17	3.25	1.19	3.12	2.93	3.67	3.47	3.13	3.63	2.90	3.38	4.11	0.97	3.87	3.60	3.37
MnO	0.05	0.06	0.05	0.06	0.04	0.09	0.03	0.01	0.03	0.02	0.06	0.05	0.08	0.06	0.06	0.06	0.05	0.06	0.07	0.02	0.07	0.06	0.05
MgO	1.56	1.42	1.42	1.02	0.64	2.39	0.66	0.43	1.34	0.35	0.99	1.00	1.70	1.32	1.53	1.35	0.99	1.31	2.30	0.21	2.11	1.41	1.29
CaO	3.60	3.51	2.66	5.29	4.14	5.91	3.24	2.03	2.24	2.52	5.29	5.10	2.92	5.04	3.52	4.86	4.00	4.69	4.55	2.10	4.74	5.00	4.35
Na_2O	4.65	4.83	5.07	4.93	4.95	4.19	6.71	6.54	5.02	5.67	4.45	4.66	5.64	4.66	4.37	5.56	4.82	4.57	6.23	6.23	5.64	5.83	4.70
K_2O	1.72	1.70	1.92	1.10	0.74	1.17	0.47	1.08	1.86	1.40	1.16	0.88	1.55	1.34	1.81	1.02	1.20	1.76	1.18	1.15	1.06	1.06	1.96
P_2O_5	0.14	0.13	0.12	0.15	0.08	0.15	0.09	0.04	0.13	0.06	0.15	0.13	0.15	0.15	0.12	0.17	0.13	0.15	0.12	0.01	0.11	0.15	0.15
LOI	1.61	1.43	1.43	0.91	0.97	1.85	0.98	1.01	2.46	1.92	1.16	1.19	1.39	1.07	1.60	0.86	0.67	0.89	0.79	0.69	0.77	0.70	0.98
Total	101.6	100.4	100.6	101.2	101.4	100.5	100.2	100.8	100.6	100.4	99.7	100.1	100.5	100.5	101.1	99.7	99.1	99.4	100.7	100.6	100.3	100.9	99.8
K_2O/Na_2O	0.37	0.35	0.38	0.22	0.15	0.28	0.07	0.16	0.37	0.25	0.26	0.19	0.27	0.29	0.41	0.18	0.25	0.38	0.19	0.19	0.19	0.18	0.42
Mg#	0.45	0.47	0.49	0.37	0.39	0.46	0.36	0.40	0.42	0.34	0.36	0.38	0.45	0.40	0.47	0.40	0.38	0.41	0.50	0.28	0.49	0.41	0.41
CIPW norm (%)																							
Quartz	23.5	23.3	24.1	21.9	29.7	18.5	22.8	25.0	25.3	27.4	23.0	24.3	18.6	26.3	21.7	17.3	25.6	21.0	13.3	30.3	16.8	16.7	21.0
Orthoclase	10.2	10.2	11.5	6.5	4.4	7.0	2.8	6.4	11.2	8.4	7.0	5.3	9.3	10.8	8.0	6.1	7.2	10.6	7.0	6.8	6.3	6.3	11.7
Albite	39.3	41.2	43.2	41.5	41.7	35.9	57.1	55.4	43.2	48.7	38.2	39.8	48.1	37.1	39.6	47.6	41.4	39.2	52.7	52.7	47.9	49.2	40.2
Anorthite	17.1	16.8	12.6	22.7	20.0	24.6	11.1	9.9	10.6	12.4	25.4	24.2	13.7	16.9	22.5	19.5	19.4	20.9	12.3	7.7	16.4	17.1	18.6
Corundum	1.99	1.31	1.83	0	0.56	0	0	0.81	2.36	0.8	0	0	1.52	1.31	0	0	0.33	0	0	0	0	0	0
Diopside	0	0	0	2.01	0	3.3	3.54	0	0	0	0.3	0.47	0	0	1.42	3.04	0	1.41	7.43	1.14	5.12	5.25	1.82
Hypersthene	3.9	3.59	3.58	1.61	1.59	4.53	0.03	1.08	3.41	0.89	2.37	2.31	4.29	3.85	2.66	2.01	2.51	2.67	2.31	0	2.93	1.09	2.42
Magnetite	0.16	0.2	0.16	0.2	0.13	0.3	0.1	0.03	0.1	0.07	0.2	0.17	0.26	0.2	0.2	0.2	0.17	0.2	0.23	0.07	0.23	0.2	0.17
Hematite	3.24	2.78	2.53	2.93	1.71	4.96	2.07	1.15	3.24	1.16	3.03	2.85	3.52	3.01	3.35	3.54	2.83	3.29	3.96	0.93	3.73	3.46	3.3
Apatite	0.31	0.29	0.26	0.33	0.17	0.33	0.2	0.09	0.29	0.13	0.33	0.29	0.33	0.26	0.33	0.38	0.29	0.33	0.26	0.02	0.24	0.33	0.33
Total	99.7	99.7	99.7	99.7	99.8	99.5	99.8	99.9	99.7	99.9	99.7	99.7	99.6	99.7	99.7	99.6	99.7	99.6	99.5	99.7	99.6	99.6	99.6

LOI = Loss on ignition.

5.3. Trace elements

The Xuelongbao rocks are depleted in HREE and variably enriched in LREE in the chondrite-normalized REE diagram (Fig. 7). Two groups of samples are identified: one rich in LREE and the other one with relatively flat LREE (Fig. 7). Martin [37] described TTG with similar REE characteristic which was interpreted as derived from typical TTG by fractional crystallization of allanite. The REE patterns of the Xuelongbao rocks may also reflect fractional crystallization of allanite. Although a few samples display slightly positive Eu anomalies which may have been produced by plagioclase accumulation, most samples do not show such anomalies (Fig. 7). In the primitive mantle-normalized trace elemental spider diagram, they show obviously negative Nb anomalies but positive Sr and Ba anomalies (Fig. 8a), similar to the pattern of the high-Si adakites (Fig. 8b). In addition, some samples show positive Zr anomalies with negative Ti anomalies (Fig. 8a).

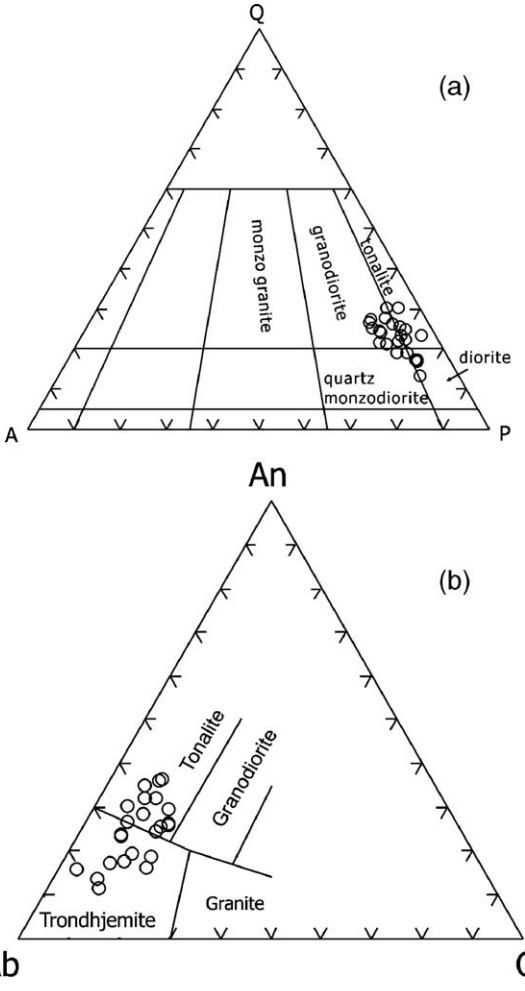

Fig. 5. Plots of (a) Q–A–P [33] and (b) An–Ab–Or [34]. The plots are based on the CIPW norm.

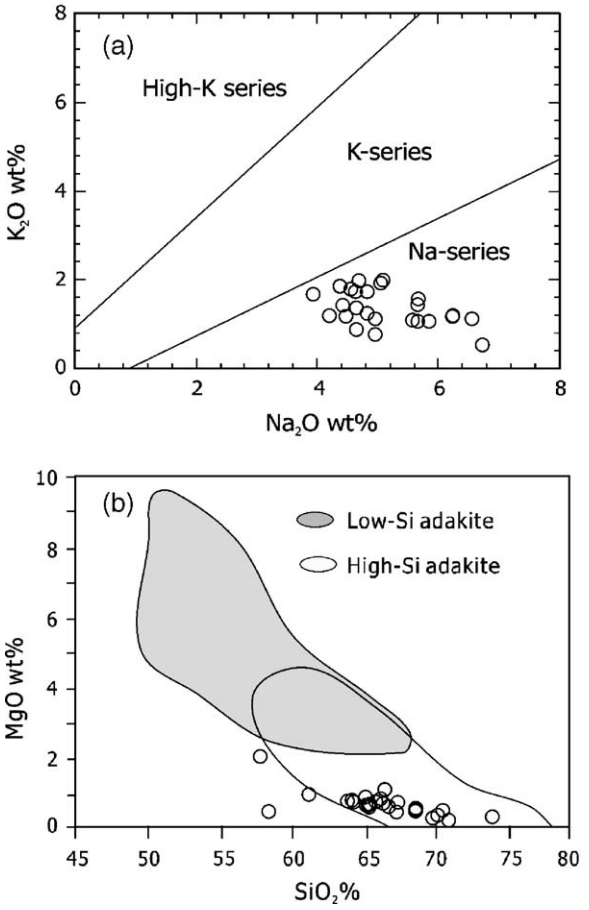

Fig. 6. Plots of (a) Na_2O vs. K_2O and (b) SiO_2 vs. MgO for the plutonic rocks from the Xuelongbao dome, SW China. Series boundaries are from Middlemost [35]. Fields of the low-Si adakites and high-Si adakites are from Martin et al. [9].

The Xuelongbao rocks have high Sr (320 to 780 ppm), low Y (<10 ppm) and high Sr/Y ratios (52–320) (Table 3) and are clearly of adakitic affinity (Fig. 9a). They are also plotted in the field of the high-Si adakites (Fig. 9b). In the trace elemental correlation diagrams (Fig. 10), again all samples are plotted in the field of the high-Si adakite. They have similar K, Rb, Nb and Ti and variable Cr/Ni ratios (Fig. 10a–d). In the Y+Nb vs. Rb diagram (Fig. 11), rocks from Xuelongbao plot in the volcanic arc field.

5.4. Rb–Sr and Sm–Nd isotopic compositions

All of the analyzed samples have clear mantle signatures with low but positive $\varepsilon Nd(t)$, ranging from +0.36 to +2.88 (Table 4). Initial $^{86}Sr/^{87}Sr$ ratios range from 0.7033 to

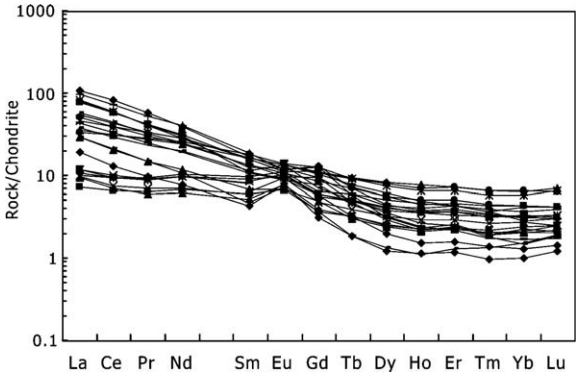

Fig. 7. Chondrite-normalized REE patterns for the plutonic rocks from the Xuelongbao dome, SW China. Normalization values are from Sun and McDonough [36].

0.7054. In the plot of εNd (*t*) vs. initial $^{86}Sr/^{87}Sr$ ratios, they are plotted near the mantle array (Fig. 12).

6. Discussion

6.1. Petrogenesis of the Xuelongbao complex

Archaean TTG suites, high-Si adakites and Phanerozoic Na-rich granitoids are relatively depleted in HREE, Y and Sc, and rich in Ba and Sr, and thus have high Sr/Y and La/Yb ratios [9,14,39]. Similarly, the plutonic rocks of the Xuelongbao complex are rich in Sr and Ba and depleted in Y and HREE (Fig. 8) and are different from the spatially associated high-K Mesozoic granites in the Songpan-Ganze Terrane [27]. Their low K_2O and high Al_2O_3 and Na_2O contents are comparable to the high-Si adakites as previously defined [9 10] (Figs. 8, 9 and 10). Thus, the plutonic rocks in the Xuelongbao dome were derived from adakitic magmas.

Although the genesis of adakitic magmas is still a matter of debate, it is generally accepted that they were derived from sources of basaltic compositions and that the presence of significant amounts of garnet±amphibole is required at some stage in the petrogenesis of these magmas, either as a residual or an early crystallizing assemblage [9,14,39–43]. Petrogenetic models for these magmas include (1) melting of a basaltic portion of the subducted oceanic lithosphere [11,12,16,44–46], (2) high-pressure fractionation of garnet and amphibole from hydrous basaltic magma [23,47], and (3) partial melting of hot mafic lower arc crust, triggered by underplating of basaltic magmas and/or release of fluids from underthrust continental rocks [21,24,41,42,48–52]. Experimental studies have suggested that melting of mafic materials produces adakitic magmas at ~ 1.2 GPa pressure, with a residual phase containing garnet but no plagioclase [40,53].

The enrichment of Sr and the absence of significant negative Eu anomalies in the Xuelongbao rocks (Figs. 7 and 8) indicate that the source was plagioclase-free. On the other hand, the depleted Y and HREE of the Xuelongbao adakitic rocks (Fig. 8) suggest the existence of garnet as a residue in the source [c.f. [11,54]], because garnet has high partition coefficients of HREE and Y relative to LREE and Sr [55]. The rocks have low Ybn (chondrite-normalized) and highly variable (La/Yb)n ratios, suggesting that the source was a hydrous amphibole eclogite or eclogite (Fig. 13). The strong depletion of both Nb and Ti in the Xuelongbao rocks suggests that the source has residual rutile and amphibole [c.f. [56]]. The element Nb tends to be hosted in amphibole, being at equilibrium with 60–70% SiO_2 melt during partial melting [57]. Ti would be hosted in rutile under hydrous mantle conditions [58]. Thus, the overall geochemical characteristics of the Xuelongbao adakite-like rocks suggest an origin by partial melting of a mafic source at pressures high enough to stabilize a residual mineral assemblage of garnet with minor amphibole.

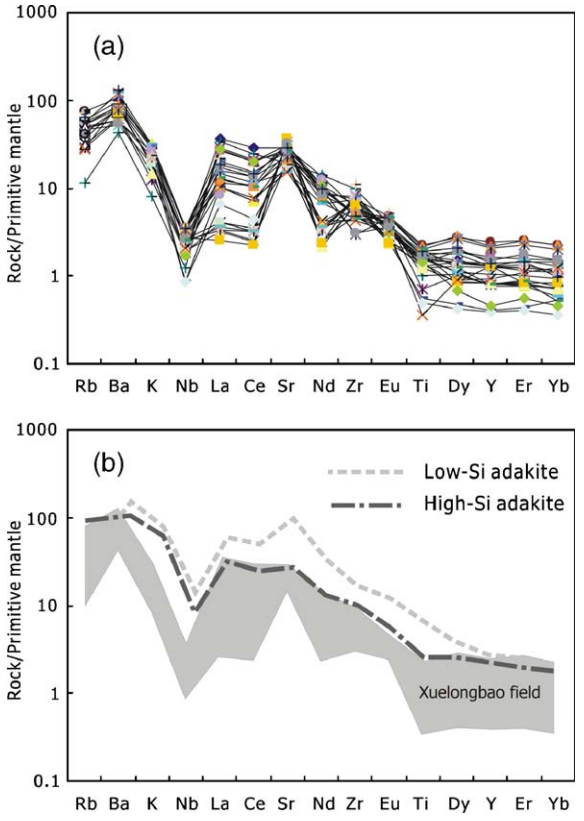

Fig. 8. Primitive mantle-normalized trace elemental spider diagram for the plutonic rocks from the Xuelongbao dome, SW China. Normalization values are from Sun and McDonough [36]. Patterns of the low-Si adakites and high-Si adakites are from Martin et al. [9].

Table 3
Trace elements and ratios of the plutonic rocks from the Xuelongbao dome, SW China

	XL-4	XL-6	XL-7	XL-19	XL-20	XL-21	XL-25	XL-26	XL-28	XL-29	XL-34	XL-35	XL-36	XL-38	XL-67	XG-1	XG-2	XG-3	XG5-1	XG5-2	XG5-3	XG-6	XG-7
Trace elements (ppm)																							
Rb	38	36	34	29	19	33	7	18	36	23	28	20	33	31	49	24	26	53	32	18	27	26	41
Ba	690	583	603	367	423	577	304	622	858	594	574	444	419	411	745	495	570	465	608	849	549	385	932
Sc	9.24	10.10	8.60	9.45	6.60	10.27	10.28	9.39	8.63	7.82	8.24	7.17	9.58	7.82	8.96	7.88	5.19	7.04	12.25	6.27	10.98	9.38	8.69
Th	5.64	3.82	1.73	0.32	4.34	0.83	4.48	1.17	1.36	0.56	0.08	0.10	0.11	0.36	3.99	0.21	5.04	0.33	2.07	2.20	2.72	3.23	2.31
U	0.48	0.64	0.62	0.55	0.21	0.20	0.27	0.21	0.18	0.07	0.21	0.25	0.29	0.53	0.70	0.49	0.86	0.67	0.94	0.62	0.94	0.78	0.27
Nb	2.00	2.48	2.57	1.83	1.31	2.02	0.86	0.60	1.26	0.60	1.32	1.37	1.80	1.79	2.44	1.72	1.18	1.95	2.35	1.48	2.35	1.85	2.47
Ta	0.14	0.19	0.34	0.10	0.06	0.10	0.04	0.03	0.04	0.03	0.06	0.06	0.08	0.14	0.23	0.11	0.08	0.10	0.19	0.13	0.21	0.18	0.11
Y	5.93	7.45	3.74	5.81	3.57	11.19	3.61	1.87	3.53	1.78	5.55	3.77	4.80	5.89	6.29	5.84	2.09	5.75	9.73	4.28	9.30	6.98	6.43
La	25	18	7	3	19	8	23	7	10	5	3	2	2	2	14	2	19	2	9	7	11	12	13
Ce	51	36	13	6	37	19	44	13	21	8	6	4	5	6	27	6	36	4	19	14	24	24	26
Pb	7.33	9.28	6.76	13.60	12.29	9.63	3.46	5.35	5.76	6.38	11.10	8.59	9.10	10.49	8.85	9.45	9.14	9.99	7.75	8.03	7.91	10.83	8.92
Sr	610	576	481	725	548	671	403	371	320	388	710	737	431	702	551	701	664	775	460	322	480	675	611
Nd	18	14	6	4	13	12	19	5	9	4	4	3	3	4	11	5	14	3	11	6	13	11	13
Zr	64	72	78	67	57	83	112	82	83	54	82	73	92	91	90	52	53	72	59	47	33	35	54
Hf	1.66	1.90	2.20	1.67	1.52	2.09	3.20	2.18	2.13	1.37	1.91	1.79	2.26	2.17	2.66	1.53	1.63	1.35	2.13	1.76	1.16	1.10	1.52
Sm	2.59	2.42	1.02	1.28	1.93	2.77	2.86	0.73	1.61	0.67	1.29	0.80	0.96	1.40	2.02	1.50	1.67	0.90	2.46	0.92	2.52	2.07	2.53
Eu	0.67	0.65	0.39	0.60	0.69	0.82	0.68	0.41	0.52	0.46	0.60	0.45	0.54	0.56	0.56	0.63	0.52	0.40	0.79	0.54	0.77	0.63	0.78
Gd	2.65	2.34	1.01	1.23	1.92	2.56	2.55	0.74	1.60	0.64	1.16	0.79	0.98	1.23	1.90	1.32	1.17	0.75	2.27	0.75	2.21	1.75	2.11
Tb	0.26	0.27	0.11	0.19	0.18	0.34	0.21	0.07	0.16	0.07	0.18	0.12	0.15	0.18	0.22	0.22	0.12	0.12	0.36	0.11	0.33	0.26	0.29
Dy	1.13	1.42	0.62	1.06	0.73	2.02	0.78	0.34	0.81	0.31	0.97	0.64	0.82	1.03	1.09	1.29	0.50	0.63	2.10	0.67	1.93	1.43	1.56
Ho	0.21	0.25	0.12	0.20	0.12	0.39	0.13	0.06	0.13	0.06	0.20	0.13	0.17	0.21	0.23	0.26	0.09	0.13	0.44	0.16	0.37	0.29	0.27
Er	0.64	0.76	0.37	0.55	0.40	1.21	0.43	0.21	0.36	0.19	0.60	0.38	0.48	0.60	0.70	0.72	0.26	0.39	1.21	0.53	1.09	0.85	0.70
Tm	0.09	0.11	0.05	0.08	0.05	0.16	0.05	0.03	0.04	0.02	0.08	0.05	0.07	0.09	0.09	0.10	0.04	0.06	0.17	0.08	0.15	0.11	0.09
Yb	0.53	0.73	0.36	0.53	0.35	1.12	0.38	0.26	0.28	0.17	0.56	0.34	0.47	0.55	0.71	0.62	0.22	0.40	1.09	0.61	0.98	0.74	0.48
Lu	0.08	0.11	0.06	0.09	0.05	0.16	0.05	0.05	0.04	0.03	0.08	0.06	0.06	0.08	0.10	0.10	0.04	0.06	0.18	0.11	0.16	0.10	0.08
Elemental ratios																							
Sr/Y	103	77	129	125	153	60	112	198	91	218	128	196	90	119	88	120	318	135	47	75	52	97	95
La/Yb	47	25	19	5	55	7	61	27	36	27	5	6	5	4	19	4	84	4	8	12	11	16	27
Th/Ce	0.11	0.11	0.14	0.05	0.12	0.04	0.10	0.09	0.07	0.07	0.01	0.02	0.02	0.06	0.15	0.04	0.14	0.08	0.11	0.16	0.11	0.13	0.09

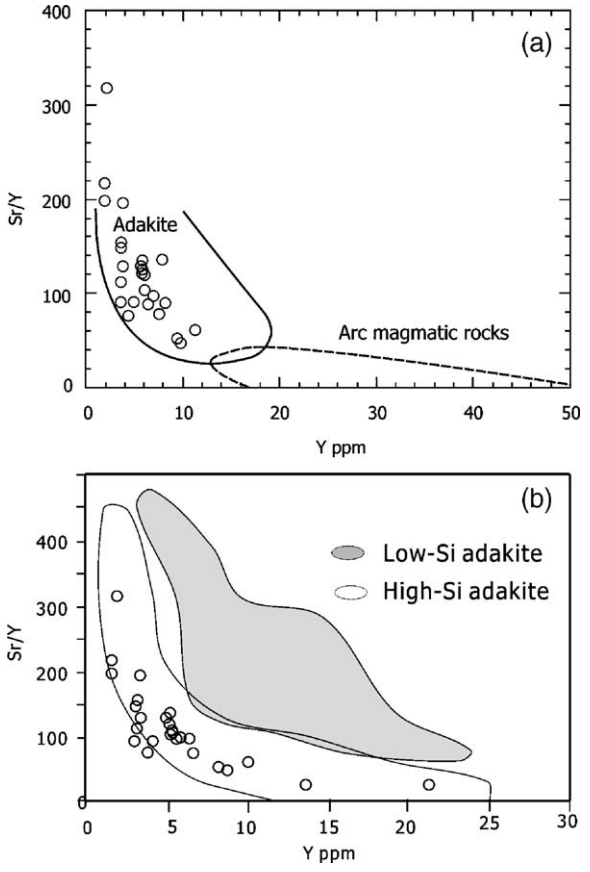

Fig. 9. Plots of Y vs. Sr/Y for the plutonic rocks from the Xuelongbao dome, SW China, showing adakitic affinity for these rocks. Fields of the low-Si adakites and high-Si adakites are from Martin et al. [9].

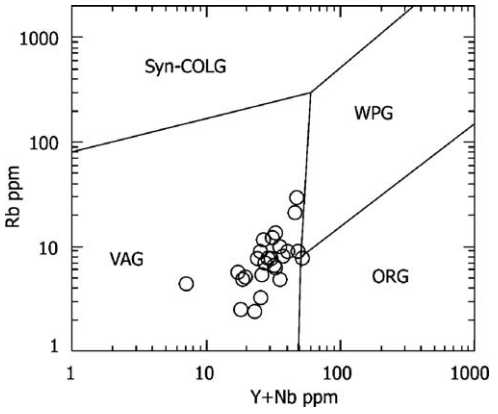

Fig. 11. Plot of Y+Nb vs. Rb for the plutonic rocks from the Xuelongbao dome, SW China. Reference fields are from Pearce et al. [38]. Syn-COLG = Syn-collisional Granite; WPG = Within Plate Granite; ORG = Orogenic granites; and VAG = Volcanic arc granite.

The low K_2O (<2 wt.%) of the Xuelongbao rocks are consistent with their derivation from magmas formed by melting of mafic rocks. The low initial $^{87}Sr/^{86}Sr$ ratios and positive εNd (*t*) values (Fig. 12) and the lack of older xenolithic zircons imply that there was no older continental components in the Xuelongbao pluton genesis and that this pluton must have directly or indirectly derived from the mantle. These isotopic compositions of Xuelongbao rocks are distinctly different from those of Late Triassic syn-collisional crust-derived granites in the Songpan-Ganze Terrane [[59] and references therein] [Fig. 1]. Thus the isotopic signatures also support an origin by melting of mafic rocks for the Xuelongbao rocks.

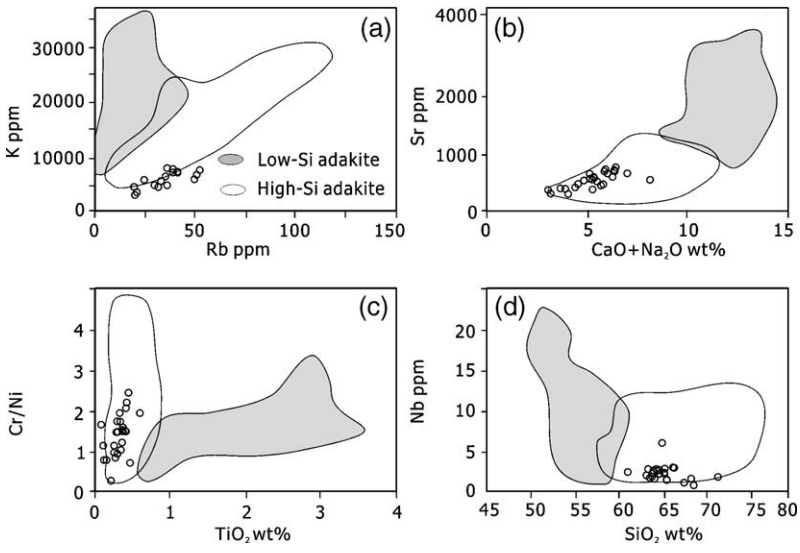

Fig. 10. Plots of (a) Rb vs. K; (b) $CaO+Na_2O$ vs. Sr; (c) TiO_2 vs. Cr/Ni ratios and (d) SiO_2 vs. Nb for the plutonic rocks from the Xuelongbao dome, SW China. Fields of the low-Si adakites and high-Si adakites are from Martin et al. [9].

Table 4
Rb–Sr and Sm–Nd isotopic compositions of the plutonic rocks from the Xuelongbao dome, SW China

Sample	Rb (ppm)	Sr (ppm)	$^{87}Rb/^{86}Sr$	$^{87}Sr/^{86}Sr$	2δ	$^{87}Sr/^{86}Sri$	Sm (ppm)	Nd (ppm)	$^{147}Sm/^{144}Nd$	$^{143}Nd/^{144}Nd$	2δ	εNd
XG-1	23.978	733.282	0.094581	0.704866	0.000014	0.70473	1.271	4.223	0.181977	0.512683	0.000012	1.065975
XG-3	46.023	753.026	0.176795	0.705677	0.000018	0.70543	1.152	4.165	0.167280	0.512637	0.000015	0.356037
XL-4	38.539	656.657	0.168150	0.705447	0.000012	0.70365	3.028	21.750	0.084285	0.512215	0.000013	2.542172
XL-7	43.356	500.431	0.251249	0.706296	0.000010	0.70361	1.008	5.689	0.107309	0.512345	0.000013	2.867850
XL-19	28.904	734.713	0.113882	0.704981	0.000013	0.70376	1.257	4.299	0.177056	0.512689	0.000021	2.878839
XL-20	19.146	564.297	0.098344	0.705267	0.000012	0.70421	2.047	13.913	0.089068	0.512228	0.000013	2.334170
XL-28	35.403	332.406	0.308779	0.706604	0.000011	0.70330	1.686	9.485	0.107634	0.512285	0.000013	1.660747
XL-39	47.120	591.190	0.231265	0.706264	0.000016	0.70379	6.452	20.594	0.189652	0.512746	0.000013	2.792548

6.2. Tectonic setting of the Xuelongbao adakitic complex

Partial melting of subducted oceanic slab is widely accepted for adakite generation, because the geochemical signatures of adakite suggest a basaltic source transformed into garnet amphibolite and amphibole eclogite [11,44,60]. However, both partial melting of a mafic lower crust under eclogite-facies conditions and slab melting can generate adakitic magmas [11,13,25,46,54,61,62]. The geochemistry of the Xuelongbao complex is consistent with slab melting as indicated by the high Na_2O contents (Table 2 and Fig 6a).

Compared with experimental melts of basalts and amphibolites, the Xuelongbao rocks have high Mg# (0.34–0.50), reflecting interactions between adakitic melt and peridotite [9,63]. The source for the Xuelongbao rocks was thus likely located under the mantle wedge, in favour of an origin by subducted slab melting.

Most melting experiments on K-poor, MORB-like compositions yielded partial melts with low K_2O (mostly <1.2 wt.%) and K_2O/Na_2O ratios (mostly <0.25) at pressures between 1 and 2 GPa and temperatures ≤ 1000 °C, regardless of the amount of H_2O present in the system [47,53,64–67]. Melts produced in such basaltic systems are granodioritic in composition. The Xuelongbao rocks have similarly low K and low K_2O/Na_2O ratios (Table 2) and are hence interpreted to have derived from partial melts of MORB-like mafic rocks.

Most of the Xuelongbao samples have Rb/Sr ratios between Cenozoic adakites and Archaean TTG suites and have lower La/Ce ratios than adakitic rocks in Eastern China (Fig. 14). Adakites from a lower crust tend to be K-richer and are distinguished by markedly higher contents of strongly incompatible elements, such as Rb, Ba, Th, and U than LREE [20–22,24,25]. The low Th and low Th/La ratios of the Xuelongbao rocks are also comparable to slab melting-derived adakites and different from lower crust-derived high-K adakites (Fig. 15a and b). Therefore, the Xuelongbao complex can be considered as formed in a subduction-related environment.

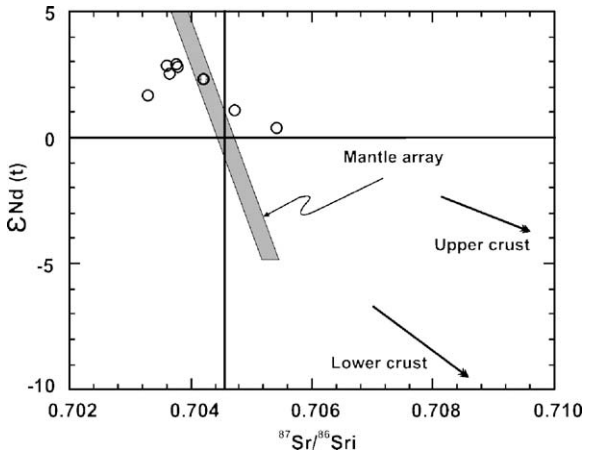

Fig. 12. Plot of initial $^{87}Sr/^{86}Sr$ vs. εNd (*t*) for the plutonic rocks from the Xuelongbao dome, SW China.

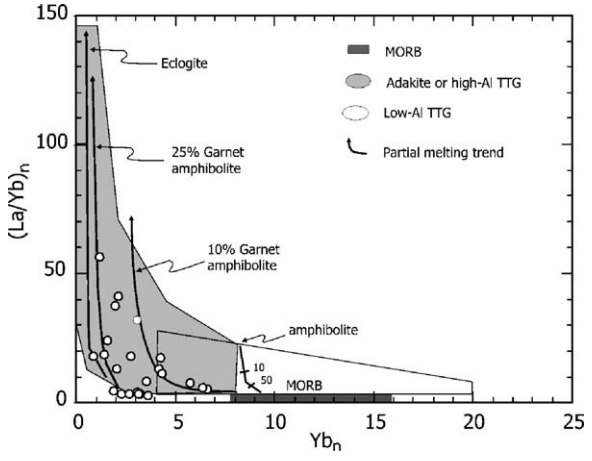

Fig. 13. Plot of Ybn vs. La/Ybn (chondrite-normalized values) for plutonic rocks from the Xuelongbao dome, SW China.

6.3. Implication for the origin of the Jinningian magmatic event

It is commonly accepted that the eastern part of the Tibetan Plateau has the same crystalline basement as the Yangtze Block [27,28]. The thick Triassic Xikang Group in the Songpan-Ganze Terrane was deposited on the continental basement of South China [28,71]. The basement rocks of the Yangtze Block are exposed as a series of domes along the eastern margin of the Songpan-Ganze Terrane, such as the Jianglong, Gezong and Gongcai domes [6,26]. The Xuelongbao dome in Longmenshan is an additional example. The new SHRIMP zircon age of 748±7 Ma obtained in this study confirms that the Xuelongbao plutonic complex crystallized during Neoproterozoic. Together with the metamorphosed Mesoproterozoic strata, it forms part of the Neoproterozoic basement complex of the Yangtze Block.

Exhumation of the crystalline basement of the Yangtze Block is related to a phase of southeast–northwest extension, as shown by the orientation of the detachment faults [6,26]. This extensional deformation, which thinned and locally removed the Palaeozoic strata overlying the basement, occurred at 166–173 Ma and was associated with post-orogenic I-type granitic magmatism in the Songpan-Ganze Terrane [6,26]. In the northern part, the linear belt was cut by the Xianshuihe strike slip fault and thus follows a curved path running from NE, to West and eventually to NW (Fig. 1).

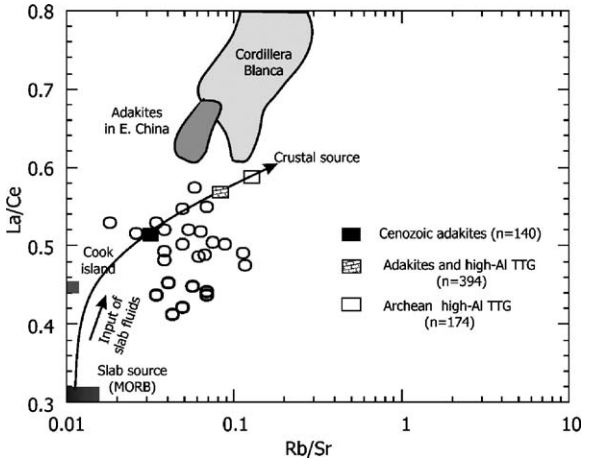

Fig. 14. Plots of Rb/Sr vs. La/Ce for the plutonic rocks from the Xuelongbao dome, SW China. Reference fields for Adakites in E. China from Xu et al. [20] and quatz–diorite and tonalite in the Cordillera Blanca from Petford and Atherton [68]. Data for Cook Island adakite derived from oceanic slab are from [69]. Cenozoic slab-derived adakites (n=140), adakite and high Al TTG (n=394) and Archaean high Al TTG (n=174) derived from lower crust are from [70].

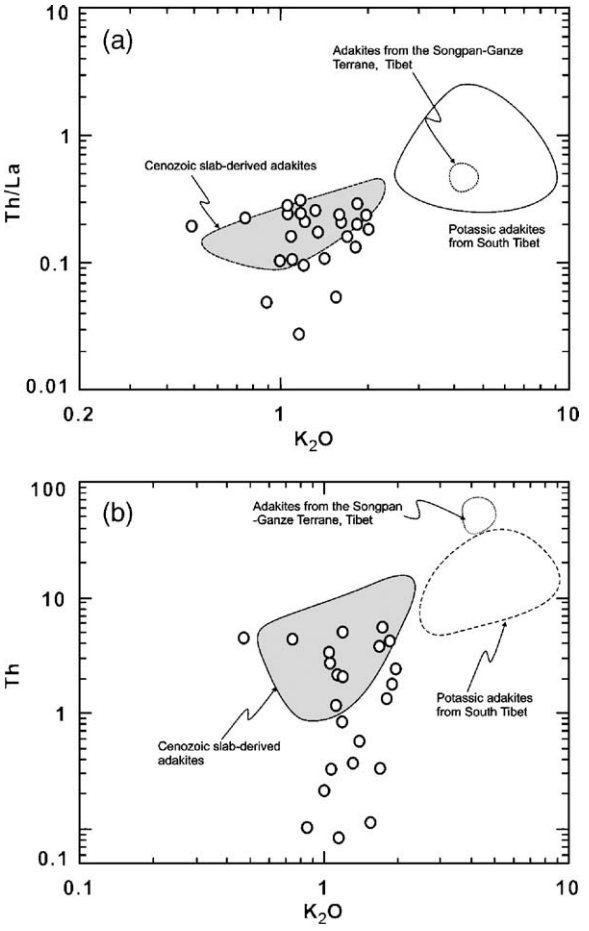

Fig. 15. Plots of (a) K_2O vs. Th and (b) K_2O vs. Th/Ce ratios for plutonic rocks from the Xuelongbao dome, SW China. Field of Cenozoic lower crust-derived adakites in the Songpan-Ganze Terrane are from Wang et al. [25], that of the patassic adakites from South Tibet from Hou et al. [22] and that of Cenozoic slab-derived adakites from Stern and Kilian [69].

Extensive Neoproterozoic (Jinningian) intermediate to silicic magmatism in South China ranges in age from 750 to 860 Ma and its origin has long been a matter of debate. Li et al. [2,3] suggested that the magmatism was produced by a mantle plume that caused the break-up of Rodinia. On the other hand, Guo et al. [4] and Wang et al. [5] considered the magmatism in the eastern part of the Yangtze Block to be post-orogenic. In the western margin of the Yangtze Block, Zhou et al. [6–8] recognized arc signatures in the mafic intrusions and granitic plutons that define the Hannan-Panxi arc. Li et al. [72] argued that the igneous rocks reported by Zhou et al. [6,7] represent rift related magmatism, and that the subduction-related geochemistry is a relict of 950 Ma Grenvillian processes. Although there are ~ 1000 Ma ophiolites and temporally associated adakites in the eastern part of the Yangtze Block [73], ophiolites and

adakites of this age are not known in the western part of the Yangtze Block. Instead, both mafic and acid intrusions range in ages from 750 to 860 Ma and are documented to be subduction-related and to define the Neoproterozoic Hannan-Panxi arc [6–8].

Occurrences of adakites have been considered to be excellent tectonic indicators [16]. The Xuelongbao complex is composed of adakitic rocks with characteristics of slab-melting in a subduction-related environment. Although the extent of adakitic rocks in a regional scale is currently unknown, an arc setting of the Xuelongbao complex (Fig. 11) provides additional insight into the nature of the Jinningian magmatism along the western margin of the Yangtze Block.

Modern adakite-high-Mg andesite-Nb-enriched basalt associations are commonly related to the subduction of young (≤20–30 Ma), hot oceanic slabs [74]. In order to allow basalt melting, H_2O must be available in such environments. Partial melting of such slabs usually requires lower temperatures (>700 °C) at depths of 75–85 km [44,60,61,75]. Slab melting can only occur under these conditions, regardless of whether subduction occurs at normal dips (10° to 30°) or at shallower angles [61,75–77]. The formation of the Xuelongbao complex is therefore consistent with previously suggested easternward (present day orientation) subduction of oceanic lithosphere underneath the Yangtze Block [6].

The adakitic rocks in Xuelongbao resemble those in the Andes [16,69,78], suggesting that the western margin of the Yangtze Block was an Andean type of continental margin during Neoproterozoic time. Therefore, our identification of adakitic rocks in the 750 Ma Xuelongbao complex provides constraints on the origin of the giant Neoproterozoic magmatism in a subduction-related environment.

7. Conclusions

The 750 Ma plutonic rocks of the Xuelongbao dome have an adakitic affinity and are part of the extensive Neoproterozoic igneous assemblage in South China. These rocks were derived from oceanic slab melting. Together with arc signatures of other granites and mafic intrusions in the region, they indicate a subduction-related environment, rather than intraplate riftings, for the Jinningian magmatism of South China.

Acknowledgments

The work described in this paper was substantially supported by research grants from the Research Grant Council of the Hong Kong SAR, China (P7124/02P) and also from the National Natural Science Foundation of China (project 40472106). We thank Ms. Christina Y. Wang and Mr. Junhong Zhao for helping with the preparation of this manuscript and Ms. Xiao Fu with the sample analyses. Reviews by Richard Ernst and an anonymous referee are gratefully acknowledged.

References

[1] B.F. Mish, The Sinian strata in the eastern Yunnan Province, Bull. Geol. Soc. China 16 (1942) 1–12.
[2] Z.X. Li, L. Zhang, C.M. Powell, South China in Rodinia: part of the missing link between Australia–East-Antarctica and Laurentia, Geology 23 (1995) 407–410.
[3] Z.X. Li, X.H. Li, P. Kinny, J. Wang, The breakup of Rodinia: did it start with a mantle plume beneath South China, Earth Planet. Sci. Lett. 173 (1999) 171–181.
[4] L.Z. Guo, Y.S. Shi, R.S. Ma, The Geotectonic Framework and Crustal Evolution of South China: Scientific Paper on Geology for International Exchange, Geological Publishing House, Beijing, 1980 (in Chinese, with English Abstract).
[5] X.L. Wang, J.C. Zhou, J.S. Qiu, J.F. Gao, Geochemistry of the Meso- to Neoproterozoic basic-acid rocks from Hunan Province, South China: implications for the evolution of the western Jiangnan orogen, Precambrian Res. 135 (2004) 79–103.
[6] M.F. Zhou, D.P. Yan, A.K. Kennedy, Y.Q. Li, J. Ding, SHRIMP zircon geochronological and geochemical evidence for Neoproterozoic arc-related magmatism along the western margin of the Yangtze Block, South China, Earth Planet. Sci. Lett. 196 (2002) 51–67.
[7] M.F. Zhou, A.K. Kennedy, M. Sun, J. Malpas, C.M. Lesher, Neo-proterozoic arc-related mafic intrusions in the northern margin of South China: implications for accretion of Rodinia, J. Geol. 110 (2002) 611–618.
[8] M.F. Zhou, Y.X. Ma, D.P. Yan, X.P. Xia, J.H. Zhao, M. Sun, The Yanbian Terrane (Southern Sichuan Province, SW China): a Neoproterozoic arc assemblage in the western margin of the Yangtze Block, Precambrian Res. 144 (2006) 19–38.
[9] H. Martin, R.H. Smithies, R. Rapp, J.F. Moyen, D. Champion, An overview of adakite, tonalite–trondhjemite–granodiorite (TTG), and sanukitoid: relationships and some implications for crustal evolution, Lithos 79 (2005) 1–24.
[10] H. Rollinson, H. Martin, Geodynamic controls on adakite, TTG and sanukitoid genesis: implications for models of crust formation, Lithos 79 (2005) 9–12.
[11] M.J. Defant, M.S. Drummond, Derivation of some modern arc magmas by the melting of young subducted lithosphere, Nature 347 (1990) 6625.
[12] M.J. Defant, M.S. Drummond, Mount St Helens: potential example of the partial melting of the subducted lithosphere in a volcanic arc, Geology 21 (1993) 547–550.
[13] H. Martin, The adakitic magmas: modern analogues of Archaean granitoids, Lithos 46 (1999) 411–429.
[14] R.H. Smithies, The Archaean tonalite–trondhjemite–granodiorite (TTG) series is not an analogue of Cenozoic adakite, Earth Planet. Sci. Lett. 182 (2000) 115–125.
[15] M.J. Defant, J.F. Xu, P. Kepezhinskas, Q. Wang, Q. Zhang, L. Xiao, Adakites: Some variations on a theme, Acta Pet. Sin. 18 (2002) 129–142.
[16] R.W. Kay, S.M. Kay, Andean adakites: three ways to make them, Acta Pet. Sin. 18 (2002) 303–311.

[17] G. Topuz, R. Altherr, W.H. Schwarz, W. Siebel, M. Satýr, A. Dokuz, Post-collisional plutonism with adakite-like signatures: the Eocene Saraycık granodiorite (Eastern Pontides, Turkey), Contrib. Mineral. Petrol. 150 (2005) 441–455.
[18] J. Bourgois, H. Martin, Y. Lagabrielle, J. LeMoigne, J.F. Jara, Subduction erosion related to spreading-ridge subduction: Taitao peninsula (Chile margin triple junction area), Geology 24 (1996) 723–726.
[19] J. Hansen, K.P. Skjerlie, R.B. Pedersen, J. De La Rosa, Crustal melting in the lower parts of island arcs: an example from the Bremanger Granitoid Complex, west Norwegian Caledonides, Contrib. Mineral. Petrol. 143 (2002) 316–335.
[20] J.F. Xu, R. Shinjio, M.J. Defant, Q. Wang, R.P. Rapp, Origin of Mesozoic adakitic intrusive rocks in the Ningzhen area of east China: partial melting of delaminated lower continental crust? Geology 32 (2002) 1111–1114.
[21] S.L. Chung, D.Y. Liu, J.Q. Ji, M.F. Chu, H.Y. Lee, D.J. Wen, C.H. Lo, T.Y. Lee, Q. Qian, Q. Zhang, Adakites from continental collision zones: melting of thickened lower crust beneath southern Tibet, Geology 31 (2003) 1021–1024.
[22] Z.Q. Hou, Y.F. Gao, X.M. Qu, Z.Y. Rui, X.X. Mo, Origin of adakitic intrusives generated during mid-Miocene east–west extension in southern Tibet, Earth Planet. Sci. Lett. 220 (2004) 139–155.
[23] Y. Takahashi, S.I. Kagashima, M.U. Mikoshiba, Geochemistry of adakitic quartz diorite in the Yamizo Mountains, central Japan: implications for Early Cretaceous adakitic magmatism in the inner zone of southwest Japan, Isl. Arc 14 (2005) 150–164.
[24] W.L. Xu, Q.H. Wang, D.Y. Wang, J.H. Guo, F.P. Pei, Mesozoic adakitic rocks from the Xuzhou-Suzhou area, eastern China: Evidence for partial melting of delaminated lower continental crust, J. Asian Earth Sci. (in press).
[25] Q. Wang, F. McDermott, J.F. Xu, H. Bellon, Y.T. Zhu, Cenozoic K-rich adakitic volcanic rocks in the Hohxil area, northern Tibet: lower-crustal melting in an intracontinental setting, Geology 33 (2005) 465–468.
[26] D.P. Yan, M.F. Zhou, H. Song, Z. Fu, Structural style and tectonic significance of the Jianglang dome in the Eastern Margin of the Tibetan Plateau, China, J. Struct. Geol. 25 (2003) 765–779.
[27] SBGMR (Sichuan Bureau of Geology and Mineral Resources), Regional geology of Sichuan Province, Geological Publishing House, Beijing, 680 pp. (in Chinese).
[28] B.C. Burchfiel, Z. Chen, Y. Liu, L.H. Royden, Tectonics of the Longmenshan and adjacent regions, central China, Int. Geol. Rev. 37 (1995) 661–736.
[29] A. Yin, T.M. Harrison, Geologic evolution of the Himalayan–Tibetan orogen, Annu. Rev. Earth Planet. Sci. 28 (2000) 211–280.
[30] W. Compston, I.S. Williams, C. Meyer, U–Pb geochronology of zircons from Lunar Breccia 73217 using a sensitive high mass-resolution ion microprobe, J. Geophys. Res. 89 (1984) 525–534.
[31] L. Qi, J. Hu, D.C. Gregoire, Determination of trace elements in granites by inductively coupled plasma-mass spectrometry, Talanta 51 (2000) 507–513.
[32] H.F. Zhang, M. Sun, F.X. Lu, X.M. Zhou, M.F. Zhou, Y.S. Liu, G.H. Zhang, Moderately depleted lithospheric mantle underneath the Yangtze Block: evidence from a garnet lherzolite xenolith in the Dahongshan kimberlite, Geochem. J. 35 (2001) 315–331.
[33] A. Streckeisen, To each plutonic rock its proper name, Earth Sci. Rev. 12 (1976) 1–33.
[34] J.T. O'Connor, A classification for quartz-rich igneous rocks based on feldspar ratio, U.S. Geol. Surv. Prof. Pap. 525-B (1976) 79–84.
[35] E.A. Middlemost, A contribution to the nomenclature and classification of volcanic rocks, Geol. Mag. 117 (1975) 7–51.
[36] S.S. Sun, W.F. McDonough, Chemical and isotopic systematics of oceanic basalts: implications for mantle composition and processes, in: A.D. Saunders, M.J. Norry (Eds.), Magmatism in the Ocean Basins, Geol. Soc. Spe. Publ., vol. 42, 1989, pp. 313–345.
[37] H. Martin, Evolution in composition of granitic-rocks controlled by time-dependent changes in petrogenetic processes — examples from the Archean of Eastern Finland, Precambrian Res. 35 (1987) 257–276.
[38] J.A. Pearce, N.B.W. Harris, A.G. Tindle, Trace-element discrimination diagrams for the tectonic interpretation of granitic-rocks, J. Petrol. 25 (1984) 956–983.
[39] K.C. Condie, TTGs and adakites: are they both slab melts? Lithos 80 (2005) 33–44.
[40] R.P. Rapp, N. Shimizu, M.D. Norman, G.S. Applegate, Reaction between slab-derived melts and peridotite in the mantle wedge: experimental constraints at 3.8 GPa, Chem. Geol. 160 (1999) 335–356.
[41] G.P. Yumul, C.B. Dimalanta, H. Bellon, D.V. Faustino, J.V. De Jesus, R.A. Tamayo, F.T. Jumawan, Adakitic lavas in the Central Luzon back-arc region, Philippines: lower crustal partial melting products? Isl. Arc 9 (2000) 499–512.
[42] J.M. Garrison, J.P. Davidson, Dubious case for slab melting in the Northern volcanic zone of the Andes, Geology 31 (2003) 565–568.
[43] G. Prouteau, B. Scaillet, M. Pichavant, R. Maury, Evidence for mantle metasomatism by hydrous silicic melts derived from subducted oceanic crust, Nature 410 (2001) 197–200.
[44] S.M. Peacock, T. Rusher, A.B. Thompson, Partial melting of subducting oceanic crust, Earth Planet. Sci. Lett. 121 (1994) 224–227.
[45] M.S. Drummond, M.J. Defant, A model for trondhjemite–tonalite–dacite genesis and crustal growth via slab melting: Archaean to modern comparisons, J. Geophys. Res. 95 (1990) 21503–21521.
[46] S.M. Kay, V.A. Ramos, M. Marquez, Evidence in Cerro Pampa volcanic rocks of slab melting prior to ridge trench collision in southern South America, J. Geol. 101 (1993) 703–714.
[47] G. Prouteau, B. Scaillet, Experimental constraints on the origin of the 1991 Pinatubo dacite, J. Petrol. 44 (2003) 2203–2241.
[48] D.R. Smith, W.P. Leeman, Petrogenesis of Mount St. Helens dacitic magmas, J. Geophys. Res. 92 (1987) 10313–10334.
[49] M.P. Atherton, N. Petford, Generation of sodium-rich magmas from newly underplated basaltic crust, Nature 362 (1993) 144–146.
[50] C.D. Wareham, I.L. Millar, A.P.M. Vaughan, The generation of sodic granitic magmas, western Palmer Land, Antarctic Peninsula, Contrib. Mineral. Petrol. 128 (1997) 81–96.
[51] R.P. Rapp, N. Shimizu, M.D. Norman, Growth of early continental crust by partial melting of eclogite, Nature 425 (2003) 605–609.
[52] J.A. Stevenson, N.R. Daczko, G.L. Clarke, N. Pearson, K.A. Kleipeis, Direct observation of adakite melts generated in the lower continental crust, Fiordland, New Zealand, Terra Nova 17 (2005) 73–79.
[53] R.P. Rapp, E.B. Watson, Dehydration melting of metabasalt at 8–32 kbar: implications for continental growth and crust mantle recycling, J. Petrol. 36 (1995) 891–931.
[54] M.J. Defant, P. Kapezhinskas, Evidence suggests slab melting in arc magmas, EOS Trans, Am. Geophys. Union 82 (2001) 65–69.
[55] H. Rollinson, Using Geochemical Data: Evaluation, Presentation, Interpretation, Longman, Singapore, 1993.
[56] J.J. Mahoney, R. Frei, M.L.G. Tejada, X.X. Mo, P.T. Leat, Tracing the Indian ocean mantle domain through time: isotopic

results from old west Indian, east Tethyan and south Pacific seafloor, J. Petrol. 39 (1998) 1285–1306.
[57] J.A. Pearce, M.J. Norry, Petrogenetic implications of Ti, Zr, Y, and Nb variations in volcanic rocks, Contrib. Mineral. Petrol. 69 (1979) 33–47.
[58] Y. Tatsumi, Chemical characteristics of fluid phase released from a subduction lithosphere and origin of arc magma: evidence from high-pressure experiments and natural rocks, J. Volcanol. Geotherm. Res. 29 (1986) 293–309.
[59] F. Roger, N. Arnaud, S. Gilder, P. Tapponnier, M. Jolivet, M. Brunel, J. Malavieille, Z. Xu, J. Yang, Geochronological and geochemical constraints on Mesozoic suturing in east central Tibet, Tectonics 22 (2003) (Articale No. 1037).
[60] F.G. Sajona, R.C. Maury, M. Pubellier, Magmatic source enrichment by slab-derived melts in a young post-collision setting, central Mindanao (Philippines), Lithos 54 (2000) 173–206.
[61] M.J. Defant, T.E. Jackson, M.S. Drummond, J.Z. De Boer, H. Bellon, M.D. Feigenson, R.C. Maury, R.H. Stewart, The geochemistry of young volcanism throughout western Panama and southeastern Costa Rica: an overview, J. Geol. Soc. (Lond.) 149 (1992) 569–579.
[62] S.L. Chung, M.F. Chu, Y.Q. Zhang, Y.W. Xie, C.H. Lo, T.Y. Lee, C.Y. Lan, X.H. Li, Q. Zhang, Y.Z. Wang, Tibetan tectonic evolution inferred from spatial and temporal variations in post-collisional magmatism, Earth Sci. Rev. 68 (2005) 173–196.
[63] R.P. Rapp, D. Laporte, H. Martin, Interactions between the subducting slab and the mantle wedge during adakite petrogenesis: experimental constraints at 1.5–4.0 GPa, Geophys. Res. Abstr. 7 (2005) 08116.
[64] R.P. Rapp, E.B. Watson, C.F. Miller, Partial melting of amphibolite/eclogite and the origin of Archean trondhjemites and tonalites, Precambrian Res. 51 (1991) 1–25.
[65] K.T. Winther, R.C. Newton, Experimental melting of hydrous low-K tholeiite: evidence on the origin of Archaean cratons, Bull. Geol. Soc. Den. 39 (1991) 213–228.
[66] K.T. Winther, An experimentally based model for the origin of tonalitic and trondhjemitic melts, Chem. Geol. 127 (1996) 43–59.
[67] S. Lo´pez, A. Castro, Determination of the fluid-absent solidus and supersolidus phase relationships of MORB-derived amphibolites in the range 4–14 kbar, Am. Mineral. 86 (2001) 1396–1403.
[68] N. Petford, M. Atherton, Na-rich partial melts from newly underplated basaltic crust: the Cordillera Blanca batholith, Peru, J. Petrol. 37 (1996) 1491–1521.
[69] C.R. Stern, R. Kilian, Role of the subducted slab, mantle wedge and continental crust in the generation of adakites from the Andean Austral Volcanic Zone, Contrib. Mineral. Petrol. 123 (1996) 263–281.
[70] M.S. Drummond, M.J. Defant, P.K. Kepezhinskas, Petrogenesis of slab-derived trondhjemite–tonalite–dacite/adakite magmas, Trans. R. Soc. Edinb. Earth sci. 87 (1996) 205–215.
[71] X.Y. Song, M.F. Zhou, Z.M. Cao, P.T. Robinson, Late Permian rifting of the South China Craton caused by the Emeishan mantle plume? J. Geol. Soc. (Lond.) 161 (2004) 773–781.
[72] Z.X. Li, X.H. Li, P. Kinny, J. Wang, S. Zhang, H. Zhou, Geochronology of Neoproterozoic syn-rift magmatism in the Yangtze Craton, South China and correlations with other continents: evidence for a mantle superplume that broke up Rodinia, Precambrian Res. 122 (2003) 85–109.
[73] W.X. Li, X.H. Li, Adakitic granites within the NE Jiangxi ophiolites, South China: geochemical and Nd isotopic evidence, Precambrian Res. 122 (2003) 29–44.
[74] A. Aguillón-Robles, T. Caimus, H. Bellon, R.C. Maury, J. Cotton, J. Bourgois, F. Michaud, Late Miocene adakite and Nb-enriched basalts from Vizcaino Peninsula, Mexico: Indicators of East Pacific Rise subduction below southern Baja California, Geology 29 (2001) 531–534.
[75] P.K. Kepezhinskas, F. McDermott, M.J. Defant, F.G. Hochstaedter, M.S. Drummond, C.J. Hawkesworth, A. Koloskov, R.C. Maury, H. Bellon, Trace element and Sr–Nd–Pb isotopic constraints on a three-component model of Kamchatka arc petrogenesis, Geochim. Cosmochim. Acta 61 (1997) 577–600.
[76] F.G. Sajona, R.C. Maury, H. Bellon, J. Cotton, M.J. Defant, M. Pubellier, C. Rangin, Initiation of subduction and the generation of slab melts in western and eastern Mindanao, Philippines, Geology 21 (1993) 1007–1010.
[77] M.A. Gutscher, R. Maury, J.P. Eissen, E. Bourdon, Can slab melting be caused by flat subduction? Geology 28 (2000) 535–538.
[78] P. Samaniego, H. Martin, M. Monzier, C. Robin, M. Fornari, J.P. Eissen, J. Cotten, Temporal evolution of magmatism in the Northern Volcanic Zone of the Andes: the geology and petrology of Cayambe Volcanic Complex (Ecuador), J. Petrol. 46 (2005) 2225–2252.